

Baryon number asymmetry and dark matter in the neutrino mass model with an inert doublet

メタデータ	言語: eng 出版者: 公開日: 2022-01-07 キーワード (Ja): キーワード (En): 作成者: メールアドレス: 所属:
URL	https://doi.org/10.24517/00064642

This work is licensed under a Creative Commons Attribution-NonCommercial-ShareAlike 3.0 International License.



Baryon number asymmetry and dark matter in the neutrino mass model with an inert doublet

Shoichi Kashiwase¹ and Daijiro Suematsu²

*Institute for Theoretical Physics, Kanazawa University,
Kanazawa 920-1192, Japan*

Abstract

The radiative neutrino mass model with an inert doublet scalar has been considered as a promising candidate which can explain neutrino masses, dark matter abundance and baryon number asymmetry if dark matter is identified with the lightest neutral component of the inert doublet. We reexamine these properties by imposing all the data of the neutrino oscillation, which are recently suggested by the reactor experiments. We find that the sufficient baryon number asymmetry seems not to be easily generated in a consistent way with all the data of the neutrino masses and mixing as long as the right-handed neutrinos are kept in TeV regions. Two possible modifications of the model are examined.

¹e-mail: shoichi@hep.s.kanazawa-u.ac.jp

²e-mail: suematsu@hep.s.kanazawa-u.ac.jp

1 Introduction

The standard model (SM) is now considered to be extended on the basis of several evidences clarified by recent experiments and observations, that is, the neutrino masses and mixing [1], the existence of dark matter (DM) [2] and also the baryon number asymmetry in the Universe [3]. Although there are a lot of models which are proposed to explain these independently, it is not so easy to construct a model which can explain all of them simultaneously without causing any other phenomenological problems. If we can find such a model, it would give us crucial hints for the new physics beyond the SM. The study along this line might play a crucial role for the search of physics beyond the SM prior to the study based on purely theoretical motivation such as the gauge hierarchy problem.

The radiative neutrino mass model with an inert doublet [4] could be such a promising candidate. It is a very simple extension of the SM by an inert doublet scalar and three right-handed neutrinos only. An imposed Z_2 symmetry controls the scalar potential and forbids the tree-level neutrino masses since its odd parity is assigned to these new fields and the even parity is assigned to the SM fields. It also guarantees the stability of the lightest field with its odd parity. Thus, the lightest neutral component of the inert doublet scalar [5, 6, 7, 8, 9] or the lightest right-handed neutrino [10, 11] could play a role of DM. This feature opens a possibility for the model such that it can explain all the above-mentioned three problems on the basis of closely related physics, simultaneously. However, the model could explain only two of the three problems if the right-handed neutrino is identified with DM [12]. In this case the model is required to be extended in some way for the explanation of all three issues [13]. On the other hand, it is noticeable that the above-mentioned three problems are suggested to be consistently explained by the new fields with TeV-scale masses as long as the lightest neutral component of the inert doublet scalar is identified with DM [6]. This latter case seems very interesting and worthy for further quantitative study since the signature of the model could be seen in various ongoing or future experiments.

In this paper we reexamine this radiative neutrino mass model by fixing the parameters relevant to the neutrino masses and mixing on the basis of neutrino oscillation data including the recent results for θ_{13} given by T2K, Double Chooz, RENO and Daya Bay [14]. We proceed this study by imposing the conditions required by the DM relic abundance and its direct detection. Based on these results, we analyze what amount of the baryon

number asymmetry can be generated via thermal leptogenesis. We show that the sufficient baryon number asymmetry seems difficult to be generated consistently for the parameters that are favored by the presently known phenomenological requirements.

The remaining parts of paper are organized as follows. In section 2, we briefly review the scalar sector of the model and then discuss the constraints brought about by the DM relic abundance and the DM direct detection. Next, we fix the parameters relevant to the neutrino mass matrix to realize the neutrino oscillation data, which are also closely related to leptogenesis. In section 3, we apply them to the study of leptogenesis and estimate the baryon number asymmetry via the out-of-thermal-equilibrium decay of the lightest right-handed neutrino by solving the Boltzmann equations numerically. Conditions to generate the suitable baryon number asymmetry are discussed. Summary of the paper is given in section 4.

2 DM abundance and neutrino masses

2.1 The model and nature of its scalar sector

We consider the radiative neutrino mass model with an inert doublet scalar [4]. The model is a very simple extension of the standard model (SM) with three right-handed neutrinos N_i , and a scalar doublet η which is called the inert doublet and assumed to have no vacuum expectation value. Although both N_i and η are supposed to have odd parity of an assumed Z_2 symmetry, all SM contents are assigned by its even parity. Invariant Yukawa couplings and scalar potential related to these new fields are summarized as

$$\begin{aligned}
-\mathcal{L}_Y &= h_{ij}\bar{N}_i\eta^\dagger\ell_j + h_{ij}^*\bar{\ell}_i\eta N_j + \frac{M_i}{2}(\bar{N}_i N_i^c + \bar{N}_i^c N_i), \\
V &= \lambda_1(\phi^\dagger\phi)^2 + \lambda_2(\eta^\dagger\eta)^2 + \lambda_3(\phi^\dagger\phi)(\eta^\dagger\eta) + \lambda_4(\eta^\dagger\phi)(\phi^\dagger\eta) \\
&+ \left[\frac{\lambda_5}{2}(\phi^\dagger\eta)^2 + \text{h.c.}\right] + m_\phi^2\phi^\dagger\phi + m_\eta^2\eta^\dagger\eta,
\end{aligned} \tag{1}$$

where ℓ_i is a left-handed lepton doublet and ϕ is an ordinary Higgs doublet. All the quartic coupling constants λ_i are assumed to be real, for simplicity. We also assume that neutrino Yukawa couplings h_{ij} are written by using the basis under which both matrices for Yukawa couplings of charged leptons and for masses of the right-handed neutrinos are real and diagonal. These neutrino Yukawa couplings are constrained by the neutrino oscillation data and also the lepton flavor-violating processes such as $\mu \rightarrow e\gamma$.

In the following study, we assume the mass spectrum of the right-handed neutrinos to satisfy

$$M_1 < M_2 < M_3, \quad (2)$$

and also the flavor structure of the neutrino Yukawa couplings to be

$$\begin{aligned} h_{ei} &= 0, & h_{\mu i} &= h_i, & h_{\tau i} &= q_1 h_i, \\ h_{ej} &= h_j, & h_{\mu j} &= q_2 h_j, & h_{\tau j} &= -q_3 h_j, \end{aligned} \quad (3)$$

where $q_{1,2,3}$ are real constants. This assumption for the neutrino Yukawa couplings could reduce free parameters of the model substantially. Moreover, it can cause the favorable lepton flavor mixing as found later. We note that there remains a freedom, that is, which type structure represented by the suffix i and j in eq. (3) should be assigned to each right-handed neutrino. In the following part, we adopt two typical cases for it as follows,

$$(i) \ i = 1, 2, \ j = 3; \quad (ii) \ i = 1, 3, \ j = 2. \quad (4)$$

Now, we briefly review the scalar sector of the model [5, 6]. If we take unitary gauge and put $\phi^T = (0, \langle\phi\rangle + \frac{h}{\sqrt{2}})$ and $\eta^T = (\eta^+, \frac{1}{\sqrt{2}}(\eta_R + i\eta_I))$ where $\langle\phi\rangle \equiv \frac{-m_\phi^2}{2\lambda_1}$, the scalar potential V in eq. (1) can be written as

$$\begin{aligned} V &= \frac{1}{2}m_h^2 h^2 + \frac{1}{2}M_{\eta_R}^2 \eta_R^2 + \frac{1}{2}M_{\eta_I}^2 \eta_I^2 + M_{\eta_c}^2 \eta^+ \eta^- + \sqrt{2\lambda_1} \langle\phi\rangle h^3 \\ &+ \frac{1}{4} \left[\sqrt{\lambda_1} h^2 - \sqrt{\lambda_2} (\eta^+ \eta^- + \eta_R^2 + \eta_I^2) \right]^2 \\ &+ \frac{1}{4} h^2 \left[(2\lambda_3 + 2\sqrt{\lambda_1 \lambda_2}) \eta^+ \eta^- + (2\lambda_+ + 2\sqrt{\lambda_1 \lambda_2}) \eta_R^2 + (2\lambda_- + 2\sqrt{\lambda_1 \lambda_2}) \eta_I^2 \right], \end{aligned} \quad (5)$$

where we use the definition $\lambda_\pm = \lambda_3 + \lambda_4 \pm \lambda_5$ and

$$m_h^2 = 4\lambda_1^2 \langle\phi\rangle^2, \quad M_{\eta_c}^2 = m_\eta^2 + \lambda_3 \langle\phi\rangle^2, \quad M_{\eta_R}^2 = m_\eta^2 + \lambda_+ \langle\phi\rangle^2, \quad M_{\eta_I}^2 = m_\eta^2 + \lambda_- \langle\phi\rangle^2. \quad (6)$$

The expression of V in eq. (5) shows that the assumed vacuum is stable for

$$\lambda_1, \lambda_2 > 0, \quad \lambda_3, \lambda_+, \lambda_- > -\sqrt{\lambda_1 \lambda_2}. \quad (7)$$

We also require these quartic couplings to satisfy $|\lambda_i| < 4\pi$ so that the perturbativity of the model is guaranteed.

Since the new doublet scalar η is assumed to have no vacuum expectation value, the Z_2 symmetry is kept as the unbroken symmetry of the model. Thus, the lightest field

with the odd parity of this Z_2 is stable and then its thermal relic behaves as DM in the Universe. If it is identified with η_R here, the following condition should be satisfied

$$\lambda_4 + \lambda_5 < 0, \quad \lambda_5 < 0; \quad M_{\eta_R} < M_1, \quad (8)$$

These are easily found from eq. (6). The value of λ_1 might be estimated by using $m_h \simeq 125$ GeV, which is suggested through the recent LHC experiments. If we apply it to the tree-level formula in eq. (6), we have $\lambda_1 \sim 0.1$. Using this value of λ_1 and the conditions given in eqs. (7) and (8), we can roughly estimate the allowed range of $\lambda_{3,4}$ as

$$\lambda_3 > -1, \quad 0 > \lambda_4 > -4\pi, \quad (9)$$

for the sufficiently small values of $|\lambda_5|$. The lower bound of λ_4 is settled by the requirement for the perturbativity of the model.

The mass difference among the components of η is estimated as

$$\frac{M_{\eta_I} - M_{\eta_R}}{M_{\eta_R}} \simeq \frac{|\lambda_5| \langle \phi \rangle^2}{M_{\eta_R}^2} \equiv \frac{\delta}{M_{\eta_R}}, \quad \frac{M_{\eta_c} - M_{\eta_R}}{M_{\eta_R}} \simeq \frac{|\lambda_4 + \lambda_5| \langle \phi \rangle^2}{2M_{\eta_R}^2}, \quad (10)$$

which could be a good approximation for the large value of m_η such as $O(1)$ TeV.³ These formulas show that coannihilation among the components of η could play an important role in the estimation of the relic abundance of η_R [6].

2.2 Inert doublet dark matter

In several articles [5], the DM abundance is found to be well explained if the lightest neutral component of η is identified with DM. In the high-mass η case, in particular, it is suggested that the relic abundance could be a suitable value if one of the quartic couplings $|\lambda_i|$ in eq. (1) has magnitude of $O(1)$ [6].

The η_R relic abundance is known to be estimated as [15]

$$\Omega_{\eta_R} h^2 \simeq \frac{1.07 \times 10^9 \text{GeV}^{-1}}{J(x_F) g_*^{1/2} m_{\text{pl}}}, \quad (11)$$

where the freeze-out temperature $T_F (\equiv M_{\eta_R}/x_F)$ and $J(x_F)$ are defined as

$$x_F = \ln \frac{0.038 m_{\text{pl}} g_{\text{eff}} M_{\eta_R} \langle \sigma_{\text{eff}} v \rangle}{(g_* x_F)^{1/2}}, \quad J(x_F) = \int_{x_F}^{\infty} \frac{\langle \sigma_{\text{eff}} v \rangle}{x^2} dx. \quad (12)$$

³Such a large value of m_η is favored from the analysis of the T parameter for the precise measurements in the electroweak interaction [5, 6]. In that case, the model has no constraint from it.

The effective annihilation cross section $\langle\sigma_{\text{eff}}v\rangle$ and the effective degrees of freedom g_{eff} are expressed by using the thermally averaged (co)annihilation cross section $\langle\sigma_{ij}v\rangle$ and the η_i equilibrium number density $n_i^{\text{eq}} = \left(\frac{M_{\eta_i}T}{2\pi}\right)^{3/2} e^{-M_{\eta_i}/T}$ as⁴

$$\langle\sigma_{\text{eff}}v\rangle = \frac{1}{g_{\text{eff}}^2} \sum_{i,j=1}^4 \langle\sigma_{ij}v\rangle \frac{n_i^{\text{eq}} n_j^{\text{eq}}}{n_1^{\text{eq}} n_1^{\text{eq}}}, \quad g_{\text{eff}} = \sum_{i=1}^4 \frac{n_i^{\text{eq}}}{n_1^{\text{eq}}}. \quad (13)$$

The thermally averaged (co)annihilation cross section may be expanded by the thermally averaged relative velocity $\langle v^2 \rangle$ of the annihilating fields as $\langle\sigma_{ij}v\rangle = a_{ij} + b_{ij}\langle v^2 \rangle$. Since $\langle v^2 \rangle \ll 1$ is satisfied for cold DM candidates and then a_{ij} gives the dominant role for determining the relic abundance of η_R , we take account of it only neglecting the b_{ij} contribution in this analysis. In the present model, the corresponding cross section is caused by the weak gauge interactions and also the quartic couplings λ_i . It is approximately calculated as [6]

$$\begin{aligned} a_{\text{eff}} &= \frac{(1 + 2c_w^4)g^4}{128\pi c_w^4 M_{\eta_1}^2} (N_{11} + N_{22} + 2N_{34}) \\ &+ \frac{s_w^2 g^4}{32\pi c_w^2 M_{\eta_1}^2} (N_{13} + N_{14} + N_{23} + N_{24}) \\ &+ \frac{1}{64\pi M_{\eta_1}^2} [(\lambda_+^2 + \lambda_-^2 + 2\lambda_3^2)(N_{11} + N_{22}) + (\lambda_+ - \lambda_-)^2(N_{33} + N_{44} + N_{12}) \\ &+ \{(\lambda_+ - \lambda_3)^2 + (\lambda_- - \lambda_3)^2\} (N_{13} + N_{14} + N_{23} + N_{24}) \\ &+ \{(\lambda_+ + \lambda_-)^2 + 4\lambda_3^2\} N_{34}], \end{aligned} \quad (14)$$

where N_{ij} is defined as

$$N_{ij} \equiv \frac{1}{g_{\text{eff}}^2} \frac{n_i^{\text{eq}} n_j^{\text{eq}}}{n_1^{\text{eq}} n_1^{\text{eq}}} = \frac{1}{g_{\text{eff}}^2} \left(\frac{M_{\eta_i} M_{\eta_j}}{M_{\eta_1}^2} \right)^{3/2} \exp \left[-\frac{M_{\eta_i} + M_{\eta_j} - 2M_{\eta_1}}{T} \right]. \quad (15)$$

Using these formulas, we examine the condition on the relevant parameters of the model to realize the relic abundance $\Omega_{\eta_R} h^2 = 0.11$ which is required from the WMAP data [2]. In Fig. 1, we plot $\Omega_{\eta_R} h^2$ as a function of λ_4 for $\lambda_5 = -10^{-5}$ and some typical values of λ_3 . We should note that the allowed region of λ_4 is restricted by eq. (9). This figure shows that the required value for $\Omega_{\eta_R} h^2$ could be obtained for a wide range value of m_η if $|\lambda_3 + \lambda_4|$ has a value of $O(1)$. Since we consider the high-mass region such as $m_\eta \gg \langle\phi\rangle$, the coannihilation among the components of η could be effective to reduce the relic abundance of η_R .

⁴We may use the notation such as $(\eta_1, \eta_2, \eta_3, \eta_4) = (\eta_R, \eta_I, \eta^+, \eta^-)$ for convenience in the following discussion.

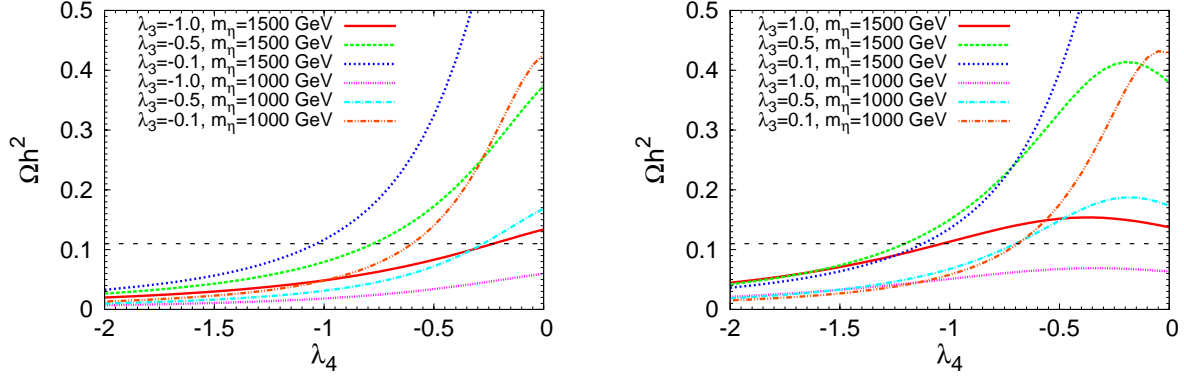


Fig. 1 $\Omega_{\eta_R} h^2$ as a function of λ_4 for the negative value of λ_3 such as -1 , -0.5 , -0.1 in the left panel and for the positive value of λ_3 such as 1 , 0.5 , 0.1 in the right panel. The value of m_η is fixed to 1000 and 1500 GeV in both cases.

The above analysis shows that the DM relic abundance gives only a weak condition on some of the quartic couplings but no conditions on the neutrino Yukawa couplings. This is completely different from the case in which the lightest N_i is identified with DM [10, 11, 12]. On the other hand, the direct search of DM could give a severe constraint on the value of λ_5 , which plays a crucial role in this radiative neutrino mass generation. Elastic scatterings between η_R and nucleus could be mediated by the Higgs exchange at tree level and also by the gauge boson exchange at one-loop level. However, their effects are much smaller than the present upper bounds of the sensitivity for the direct detection. Thus, we can neglect their effects in this discussion. On the other hand, inelastic scattering of η_R with nucleus mediated by the Z^0 exchange could bring about an important effect to the direct search experiments [8, 9], since the masses of η_R and η_I are almost degenerate for small values of $|\lambda_5|$ as found from eq. (10).

If we note that the interaction of η_R relevant to this process is given by

$$\mathcal{L} = g\eta_R\partial_\mu\eta_I Z^\mu - g\eta_I\partial_\mu\eta_R Z^\mu, \quad (16)$$

it is found that the inelastic nucleus-DM scattering can occur for the DM with velocity larger than a minimum value given by [16]

$$v_{\min} = \frac{1}{\sqrt{2m_N E_R}} \left(\frac{m_N E_R}{\mu_N} + \delta \right), \quad (17)$$

where δ is the mass difference between η_R and η_I defined in eq.(10). E_R is the nucleus recoil energy, and m_N and μ_N are the mass of the target nucleus and the reduced mass

of the nucleus-DM system. Thus, the mass difference δ is constrained by the fact that no DM signal is found in the direct DM search yet [17, 18].⁵ This condition might be estimated as $\delta \gtrsim 150$ keV [9]. Since δ is related to λ_5 through eq.(10), this constrains the allowed value of $|\lambda_5|$ such as⁶

$$|\lambda_5| \simeq \frac{M_{\eta_1} \delta}{\langle \phi \rangle^2} \gtrsim 5.0 \times 10^{-6} \left(\frac{M_{\eta_1}}{1 \text{ TeV}} \right) \left(\frac{\delta}{150 \text{ keV}} \right). \quad (18)$$

We take account of this constraint in the following analysis of the neutrino masses and the baryon number asymmetry.

2.3 Neutrino masses and mixing

Neutrino masses are generated through one-loop diagrams with the contribution of new Z_2 odd fields. They can be expressed as [4, 10]

$$\mathcal{M}_{ij}^\nu = \sum_{k=1}^3 h_{ik} h_{jk} \left[\frac{\lambda_5 \langle \phi \rangle^2}{8\pi^2 M_k M_\eta^2 - M_k^2} \left(1 + \frac{M_k^2}{M_\eta^2 - M_k^2} \ln \frac{M_k^2}{M_\eta^2} \right) \right] \equiv \sum_{k=1}^3 h_{ik} h_{jk} \Lambda_k, \quad (19)$$

where $M_\eta^2 = m_\eta^2 + (\lambda_3 + \lambda_4) \langle \phi \rangle^2$. Since we consider the high-mass region such as $m_\eta \gg \langle \phi \rangle$, the mass difference among η_i caused by nonzero λ_4 is negligible in the neutrino mass analysis. Thus, we treat their masses as M_η . Both neutrino masses and mixing are determined by the couplings λ_5 and h_{ik} , the right-handed neutrino masses M_i 's and the inert doublet mass M_η . Here we note that the neutrino Yukawa couplings could take rather large values even for the light right-handed neutrinos with masses of $O(1)$ TeV as long as $|\lambda_5|$ takes a small value in the range given by eq. (18). This freedom is crucial when we consider leptogenesis in this model as seen in the next section.

Now we have a lot of information on the feature of lepton flavor mixing on the basis of the neutrino oscillation data including the recent results for θ_{13} [19]. We can use it to restrict the neutrino Yukawa couplings. The flavor structure of the neutrino Yukawa

⁵The DAMA data have been suggested to be explained by the DM inelastic scattering [8, 9]. However, we do not consider it here.

⁶We should note that the bound of δ largely depends on the DM velocity in the neighborhood of the Earth. If we take $\delta \gtrsim 1$ MeV, this inelastic scattering effect can be completely neglected even for the maximally estimated DM velocity. In that case, the lower bound of $|\lambda_5|$ becomes one order of magnitude larger.

couplings assumed in eq. (3) makes the neutrino mass matrix take a simple form such as

$$\mathcal{M}^\nu = \begin{pmatrix} 0 & 0 & 0 \\ 0 & 1 & q_1 \\ 0 & q_1 & q_1^2 \end{pmatrix} (h_1^2 \Lambda_1 + h_i^2 \Lambda_i) + \begin{pmatrix} 1 & q_2 & -q_3 \\ q_2 & q_2^2 & -q_2 q_3 \\ -q_3 & -q_2 q_3 & q_3^2 \end{pmatrix} h_j^2 \Lambda_j, \quad (20)$$

where i, j should be understood to stand for (i) $i = 2, j = 3$ and (ii) $i = 3, j = 2$ following eq. (4). If we put $q_{1,2,3} = 1$ in both cases, the PMNS mixing matrix is easily found to have a tribimaximal form

$$U_{PMNS} = \begin{pmatrix} \frac{2}{\sqrt{6}} & \frac{1}{\sqrt{3}} & 0 \\ \frac{-1}{\sqrt{6}} & \frac{1}{\sqrt{3}} & \frac{1}{\sqrt{2}} \\ \frac{1}{\sqrt{6}} & \frac{-1}{\sqrt{3}} & \frac{1}{\sqrt{2}} \end{pmatrix} \begin{pmatrix} 1 & 0 & 0 \\ 0 & e^{i\alpha_1} & 0 \\ 0 & 0 & e^{i\alpha_2} \end{pmatrix}, \quad (21)$$

where Majorana phases $\alpha_{1,2}$ are determined by the phases h_i and λ_5 . If we put $\varphi_i = \arg(h_i)$ and $\varphi_{\lambda_5} = \arg(\lambda_5)$, they are expressed as

$$\alpha_1 = \varphi_3 + \frac{\varphi_{\lambda_5}}{2}, \quad \alpha_2 = \frac{1}{2} \tan^{-1} \left(\frac{|h_1|^2 \Lambda_1 \sin(2\varphi_1 + \varphi_{\lambda_5}) + |h_2|^2 \Lambda_2 \sin(2\varphi_2 + \varphi_{\lambda_5})}{|h_1|^2 \Lambda_1 \cos(2\varphi_1 + \varphi_{\lambda_5}) + |h_2|^2 \Lambda_2 \cos(2\varphi_2 + \varphi_{\lambda_5})} \right). \quad (22)$$

In this case, one of mass eigenvalues is zero. Thus, if $|h_1|$ is assumed to take a sufficiently small value compared with others, we find that the mass eigenvalues should satisfy

$$|h_i|^2 \Lambda_i \simeq \frac{\sqrt{\Delta m_{\text{atm}}^2}}{2}, \quad |h_j|^2 \Lambda_j \simeq \frac{\sqrt{\Delta m_{\text{sol}}^2}}{3}, \quad (23)$$

where Δm_{atm}^2 and Δm_{sol}^2 stand for the squared mass differences required by the neutrino oscillation analysis for both atmospheric and solar neutrinos [1, 19].⁷

Using the formulas (21) and (23), we can examine whether parameters obtained in the previous part could be consistent with the neutrino oscillation data. This gives a useful starting point for the analysis. However, if we take account of the fact that θ_{13} is found to have a nonzero value now, we cannot use them in the analysis directly. Here, we numerically diagonalize the mass matrix (20) and impose both the neutrino oscillation data and the constraint on $|\lambda_5|$ given in eq. (18) to restrict the neutrino Yukawa couplings. By fixing q_1 to typical values, in Fig. 2, we plot contours in the (q_2, q_3) plane which correspond to 2σ bounds of the neutrino oscillation parameters given in [20]. This figure shows the mass matrix (20) can explain all the neutrino oscillation data consistently at

⁷We confine our study to the normal hierarchy here.

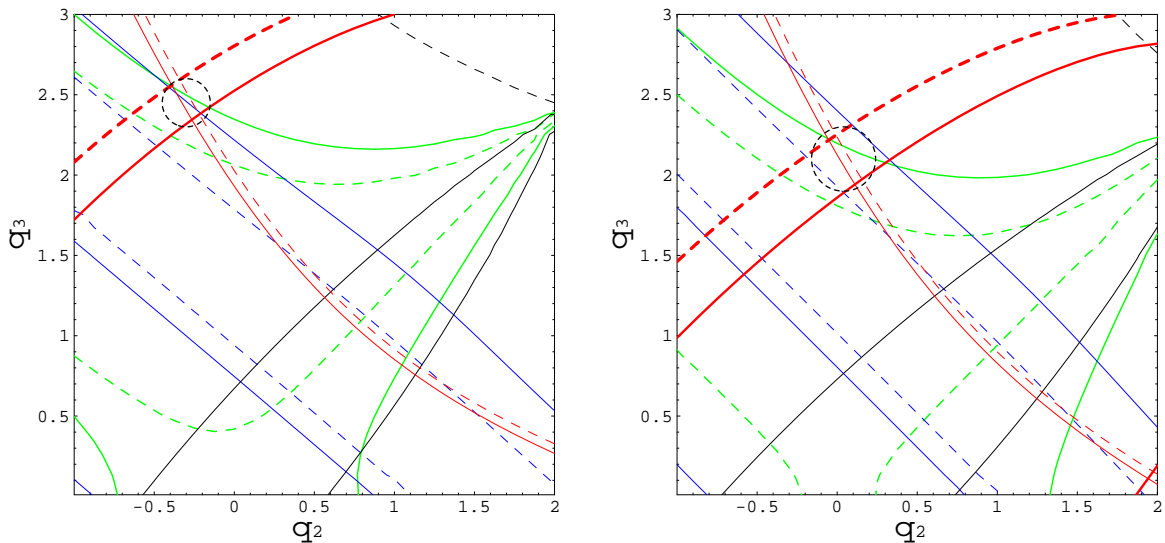


Fig. 2 Regions in the (q_2, q_3) plane allowed by the neutrino oscillation data for $q_1 = 0.85$ (left panel) and $q_1 = 1$ (right panel), which are contained in the circle drawn by the dotted line. Relevant parameters are fixed to the ones shown in Table 1. Each contour in both panels represents 2σ boundary values of neutrino oscillation parameters Δm_{32}^2 (thick red solid and dashed lines), $|\Delta m_{12}^2|$ (thin red solid and dashed lines), $\sin^2 2\theta_{23}$ (green solid and dashed lines), $\sin^2 2\theta_{12}$ (blue solid and dashed lines) which are given in Ref.[20]. The 90% CL value of $\sin^2 2\theta_{13}$ given in Ref.[14] is also plotted as a reference (black solid and dashed lines).

the regions in the (q_2, q_3) plane, which are the region including $(-0.27, 2.4)$ in the left panel ($q_1 = 0.85$) and the region including $(0.05, 2.1)$ in the right panel ($q_1 = 1$). These regions in two panels are obtained for each set of parameters listed in Table 1. We also give the predicted values for $\sin^2 2\theta_{13}$ in each case of the same Table. These examples show that neutrino Yukawa couplings of $O(10^{-3})$ can explain the neutrino oscillation data for $|\lambda_5| = O(10^{-5})$ and the right-handed neutrinos with the mass of $O(1)$ TeV.

Lepton flavor-violating processes such as $\mu \rightarrow e\gamma$ are also induced through one-loop diagrams which have η and N_i in the internal lines [10]. Their present experimental bounds could impose severe constraints on the model depending on the values of neutrino Yukawa couplings h_i . However, since the small $|h_i|$ of $O(10^{-3})$ can realize the appropriate values for neutrino masses even for the TeV-scale values of M_i and M_η as discussed above, the new contributions to the lepton flavor-violating processes are sufficiently suppressed such as $\text{Br}(\mu \rightarrow e\gamma) = O(10^{-18})$ and $\text{Br}(\tau \rightarrow \mu\gamma) = O(10^{-14})$. These values show that the lepton flavor-violating processes bring about no substantial constraints on the model.

	q_1	M_η	M_1	M_2	M_3	$10^3 h_2 $	$10^3 h_3 $	$\sin^2 2\theta_{13}$	$\max \varepsilon_{2,3} $	Y_B
(ia)	0.85	1	2	6	10	3.41	1.50	0.085	$1.1 \cdot 10^{-7}$	$2.7 \cdot 10^{-12}$
(ib)	0.85	1	2	20	200	4.62	4.16	0.085	$6.1 \cdot 10^{-8}$	$1.6 \cdot 10^{-12}$
(ic)	1	1	2	6	10	3.41	1.50	0.053	$9.8 \cdot 10^{-8}$	$2.8 \cdot 10^{-12}$
(iia)	0.85	1	2	6	10	1.34	3.81	0.085	$1.7 \cdot 10^{-8}$	$2.7 \cdot 10^{-13}$
(iib)	0.85	1	2	20	200	1.82	10.6	0.085	$9.5 \cdot 10^{-9}$	$8.3 \cdot 10^{-13}$

Table 1 The predicted value of $\sin^2 2\theta_{13}$ and Y_B for the model parameters that can satisfy the neutrino oscillation data. Cases (i) and (ii) correspond to the ones defined in eq. (4). In all cases, $|\lambda_5|$ and $|h_1|$ are fixed to 10^{-5} and $3 \cdot 10^{-8}$, respectively. The value of $\sin^2 2\theta_{13}$ is evaluated at $(q_2, q_3) = (-0.27, 2.4)$ for $q_1 = 0.85$ and $(0.05, 2.1)$ for $q_1 = 1$, where all other neutrino oscillation data are satisfied. A TeV unit is used as the mass scale.

We should note that the freedom of λ_5 in this mass generation scheme makes it possible.

3 Baryon number asymmetry

3.1 Leptogenesis via the decay of the TeV-scale right-handed neutrino

We consider the thermal leptogenesis [21] in this model with the mass spectrum given in eqs. (2) and (8). In this case, the lepton number asymmetry is expected to be generated through the out-of-thermal-equilibrium decay of the right-handed neutrino N_1 . The dominant contribution to the CP asymmetry ε in this decay is brought about by the interference between the tree diagram and the one-loop vertex diagram as usual. However, we should note that the η mass is not negligible compared with the one of N_1 in this model. Taking account of this feature, ε can be calculated as [22]

$$\begin{aligned}
\varepsilon &= \frac{1}{16\pi \left[\frac{3}{4} + \frac{1}{4} \left(1 - \frac{M_\eta^2}{M_1^2} \right)^2 \right]} \sum_{i=2,3} \frac{\text{Im} \left[\left(\sum_{k=e,\mu,\tau} h_{k1} h_{ki}^* \right)^2 \right]}{\sum_{k=e,\mu,\tau} h_{k1} h_{k1}^*} G \left(\frac{M_i^2}{M_1^2}, \frac{M_\eta^2}{M_1^2} \right) \\
&\equiv \varepsilon_2 \sin 2(\varphi_1 - \varphi_2) + \varepsilon_3 \sin 2(\varphi_1 - \varphi_3), \tag{24}
\end{aligned}$$

where $G(x, y)$ is defined by

$$G(x, y) = \frac{5}{4}F(x, 0) + \frac{1}{4}F(x, y) + \frac{1}{4}(1 - y)^2 [F(x, 0) + F(x, y)], \quad (25)$$

and $F(x, y)$ is represented as

$$F(x, y) = \sqrt{x} \left[1 - y - (1 + x) \ln \left(\frac{1 - y + x}{x} \right) \right]. \quad (26)$$

If we use the flavor structure of neutrino Yukawa couplings (i) and (ii) given in eq. (4), $\varepsilon_{2,3}$ are expressed for each case as

$$\begin{aligned} \text{(i)} \quad \varepsilon_2 &= C(1 + q_1^2) |h_2|^2 G \left(\frac{M_2^2}{M_1^2}, \frac{M_\eta^2}{M_1^2} \right), \quad \varepsilon_3 = \frac{C(q_2 - q_1 q_3)^2 |h_3|^2}{1 + q_1^2} G \left(\frac{M_3^2}{M_1^2}, \frac{M_\eta^2}{M_1^2} \right), \\ \text{(ii)} \quad \varepsilon_2 &= \frac{C(q_2 - q_1 q_3)^2 |h_2|^2}{1 + q_1^2} G \left(\frac{M_2^2}{M_1^2}, \frac{M_\eta^2}{M_1^2} \right), \quad \varepsilon_3 = C(1 + q_1^2) |h_3|^2 G \left(\frac{M_3^2}{M_1^2}, \frac{M_\eta^2}{M_1^2} \right), \end{aligned} \quad (27)$$

where $C^{-1} = 16\pi \left[\frac{3}{4} + \frac{1}{4} \left(1 - \frac{M_\eta^2}{M_1^2} \right)^2 \right]$.

The decay of N_1 should be out of equilibrium so that the lepton number asymmetry is generated through it. If we express the Hubble parameter and the decay width of N_1 by H and $\Gamma_{N_1}^D$ respectively, this condition is given as $H > \Gamma_{N_1}^D$ at $T \sim M_1$ where the lepton number asymmetry is considered to be dominantly generated. Since $\Gamma_{N_1}^D$ is expressed as $\Gamma_{N_1}^D = \frac{|h_1|^2}{8\pi} (1 + q_1)^2 M_1 \left(1 - \frac{M_\eta^2}{M_1^2} \right)^2$, we find that the Yukawa coupling $|h_1|$ should be sufficiently small such as

$$|h_1| < 2 \times 10^{-8} (1 + q_1^2)^{-1/2} \left(\frac{M_1}{1 \text{ TeV}} \right)^{1/2}. \quad (28)$$

We note that this constraint could be weaker since both M_η and the Boltzmann suppression factor are neglected in this estimation. As found in the numerical calculation, $|h_1|$ can be somewhat larger than this bound.

The generated lepton number asymmetry could be washed out by both the lepton number violating 2-2 scattering such as $\eta\eta \rightarrow \ell_\alpha \ell_\beta$ and $\eta\ell_\alpha \rightarrow \eta^\dagger \bar{\ell}_\beta$ and also the inverse decay of N_1 . If the relevant Yukawa couplings are much smaller than $O(1)$, these processes are expected to decouple before the temperature T of the thermal plasma decreases to $T \sim M_1$. In order to study this quantitatively, we numerically solve the coupled Boltzmann equations for the number density of N_1 and the lepton number asymmetry which are expressed by n_{N_1} and n_L here, respectively. The Boltzmann equations for these quantities

are written as [23]

$$\begin{aligned}\frac{dY_{N_1}}{dz} &= -\frac{z}{sH(M_1)} \left(\frac{Y_{N_1}}{Y_{N_1}^{\text{eq}}} - 1 \right) \left\{ \gamma_D^{N_1} + \sum_{i=2,3} \left(\gamma_{N_1 N_i}^{(2)} + \gamma_{N_1 N_i}^{(3)} \right) \right\}, \\ \frac{dY_L}{dz} &= \frac{z}{sH(M_1)} \left\{ \varepsilon \left(\frac{Y_{N_1}}{Y_{N_1}^{\text{eq}}} - 1 \right) \gamma_D^{N_1} - \frac{2Y_L}{Y_\ell^{\text{eq}}} \left(\gamma_N^{(2)} + \gamma_N^{(13)} \right) \right\},\end{aligned}\quad (29)$$

where $z = \frac{M_1}{T}$ and $H(M_1) = 1.66g_*^{1/2} \frac{M_1^2}{m_{\text{pl}}}$. Y_{N_1} and Y_L are defined as $Y_{N_1} = \frac{n_{N_1}}{s}$ and $Y_L = \frac{n_L}{s}$ by using the entropy density s . Their equilibrium values are expressed as $Y_{N_1}^{\text{eq}}(z) = \frac{45}{2\pi^4 g_*} z^2 K_2(z)$ and $Y_\ell^{\text{eq}} = \frac{45}{\pi^4 g_*}$, where g_* is the number of relativistic degrees of freedom and $K_2(z)$ is the modified Bessel function of the second kind. In these equations we omit terms whose contributions are considered to be negligible compared with others. The formulas of the relevant reaction density γ contained in these equations are given in the Appendix. If we use the relation $B = \frac{8}{23}(B - L)$ which is derived with the chemical equilibrium condition in this model, the baryon number asymmetry $Y_B (= \frac{n_B}{s})$ in the present Universe is found to be estimated as

$$Y_B = -\frac{8}{23} Y_L(z_{\text{EW}}) \quad (30)$$

by using the solution $Y_L(z)$ of the coupled equations in eq. (29). Here z_{EW} is related to the sphaleron decoupling temperature T_{EW} as $z_{\text{EW}} = \frac{M_1}{T_{\text{EW}}}$.

The solutions of eq. (29) are shown in the upper panels of the left and the middle columns in Fig. 3 for cases (ia) and (ib) in Table 1. The generated lepton number asymmetry $|Y_L|$ is smaller than the value required for the explanation of the baryon number asymmetry at least by one order of magnitude.⁸ In case (ia), the CP asymmetry parameter $|\varepsilon|$ takes rather large value such as $1.1 \cdot 10^{-7}$. This suggests that the washout of the generated lepton number asymmetry is effective. In the figure of the right column we use the same parameters as the one of case (ia) except for $|h_1|$ which is fixed to the larger value $5 \cdot 10^{-7}$. From this figure, we can see the role of this coupling which is discussed above. Although this change does not affect the values of $|h_{2,3}|$ which explain the neutrino oscillation data, we expect that the deviation of the number density of N_1 from the equilibrium value becomes smaller than other cases with the smaller value of $|h_1|$. This is shown in the figures.

⁸The parameters used in case (ia) are almost equivalent to the one which is presented as the promising one for the generation of the sufficient baryon number asymmetry in [6].

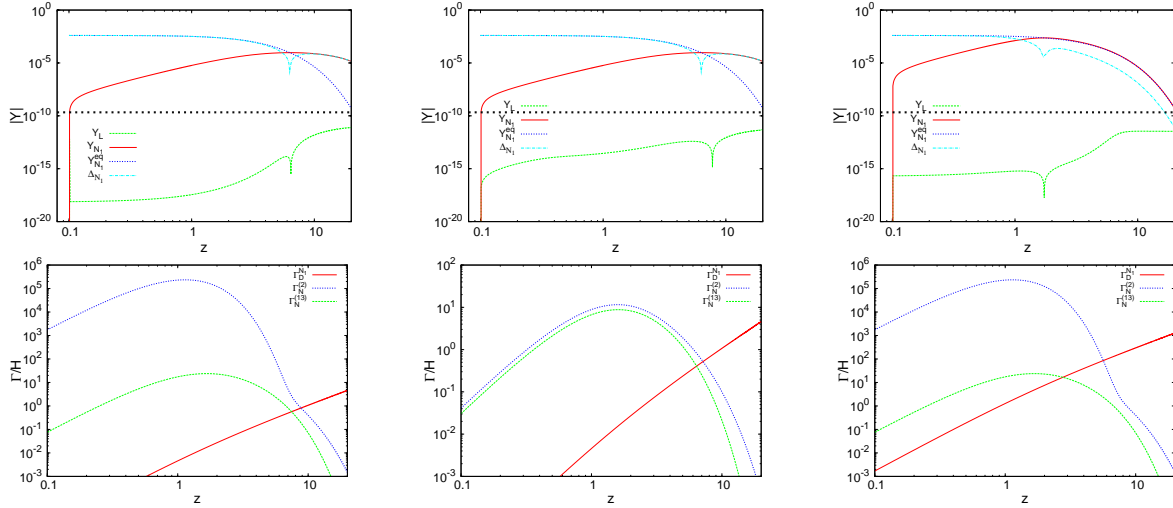


Fig. 3 The upper panels show the evolution of Y_L , Y_{N_1} and $\Delta_{N_1} \equiv |Y_{N_1} - Y_{N_1}^{\text{eq}}|$. The lower panels show the reaction rates $\frac{\Gamma}{H}$ of the processes that have crucial effects for the leptogenesis in this model. We use the parameters shown as (ia) and (ib) in Table 1 for the left and middle panels. In the right panel the same parameters as (ia) are used except for $|h_1|$, which is fixed to $|h_1| = 5 \cdot 10^{-7}$ in this case. The black dotted line represents the required value for $|Y_L|$.

In the lower panel we plot the behavior of the relevant reaction rates for each case. These processes are crucial for the leptogenesis in this model. The figures show that the lepton number-violating scatterings induced by the s -channel N_i exchange are kept in the thermal equilibrium until rather late period and the large part of the generated lepton number asymmetry is washed out. This situation is common for all cases in Table 1. We give the predicted value of Y_B for each case in the last column of Table 1. These examples show that the sufficient amount of baryon number asymmetry seems difficult to be generated through the thermal leptogenesis in the present neutrino mass generation scheme at least as long as we impose the full neutrino oscillation data and the DM direct search constraint.

In order to confirm this statement in case (ia), we plot the generated baryon number asymmetry Y_B for various values of $|\lambda_5|$ in Fig. 4. The maximum value of Y_B is found to be realized at a certain value of $|\lambda_5|$ and it moves to the smaller $|\lambda_5|$ region for the smaller M_1 . This may be explained as follows. At the region with a larger $|\lambda_5|$ value, the neutrino Yukawa couplings have smaller values to give a smaller value for $|\varepsilon|$. On the other hand, at the region with a smaller $|\lambda_5|$ value, the neutrino Yukawa couplings have larger values

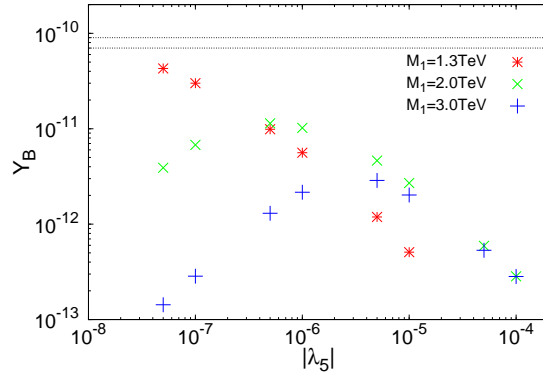


Fig. 4 The dependence of the generated baryon number asymmetry Y_B on $|\lambda_5|$ in case (ia) with the different value of M_1 . The value of M_1 is fixed to 1.3 TeV, 2 TeV and 3 TeV in each case.

to bring about the large washout. For the $M_1 = 1.3$ TeV case, the required Y_B can be obtained at a rather small value such as $|\lambda_5| \leq 10^{-6}$ due to this nature. However, it is excluded by the direct search experiments as shown in eq. (18).⁹ Although we do not search the whole parameter space, we could say that the above-mentioned result does not change so easily for the values of $|\lambda_5|$ which satisfy the condition (18). This is suggested by the fact that the value of Y_B becomes smaller for the larger $|\lambda_5|$ which makes the neutrino Yukawa couplings smaller under the constraints of the neutrino oscillation data.

Finally, we give some comments on the leptogenesis in the case where the right-handed neutrinos have large masses comparable to the ones in the ordinary seesaw case.¹⁰ In this case, we find that the DM relic abundance and the neutrino masses and mixing could be explained consistently by setting $|\lambda_5|$ and the neutrino Yukawa couplings appropriately. The right-handed neutrino masses could be smaller than the ones in the ordinary tree-level seesaw case for the same neutrino Yukawa couplings since the neutrino masses are generated through the one-loop effect. In the ordinary type I seesaw scenario with the hierarchical right-handed neutrino masses, there is an upper bound for the CP asymmetry which is known as the Davidson-Ibarra (DI) bound [25] and may be written as $|\varepsilon_{\text{DI}}| = \frac{3}{8\pi} \frac{M_1 \sqrt{\Delta m_{\text{atm}}^2}}{\langle \phi \rangle^2}$. In the present case with the assumed flavour structure, the CP asymmetry $|\varepsilon|$ is related to the DI bound as $|\varepsilon| = |\varepsilon_{\text{DI}}| \frac{\pi^2}{3 \ln(M_2/M_\eta)} \frac{1+q_1^2}{|\lambda_5|} \left(\frac{M_2}{M_1}\right)^2$. This shows that the DI

⁹It is useful to note that the smaller M_η brings about the smaller value for the lower bound of $|\lambda_5|$. However, its effect is only a change of the factor in case of the high-mass η .

¹⁰This is considered in [7]. However, the neutrino oscillation data are not imposed in a quantitative way there.

bound could be evaded depending on the value of $|\lambda_5|$. However, this feature does not mean that the model causes more efficient leptogenesis than the ordinary seesaw model. Since the smaller $|\lambda_5|$ requires the larger neutrino Yukawa couplings under the constraints of the neutrino oscillation data, the washout of the lepton number asymmetry is expected to become large.

We examine this aspect under the assumed lepton flavor structure by imposing all the neutrino oscillation data quantitatively. We assume the hierarchical right-handed neutrino mass spectrum and fix the parameters as follows,

$$|h_1| = 10^{-4}, \quad M_1 = 10^\alpha \text{ GeV}, \quad M_2 = 10^{\alpha+1} \text{ GeV}, \quad M_3 = 10^{\alpha+2} \text{ GeV}, \quad (31)$$

where $|h_1|$ is determined by taking account of the condition (28). We find that the CP asymmetry $|\varepsilon|$ can be written for these parameters as $|\varepsilon| \simeq |\varepsilon_{\text{DI}}| \frac{2.5 \cdot 10^2}{(\alpha-2)|\lambda_5|}$ where the DI bound $|\varepsilon_{\text{DI}}|$ is given as $|\varepsilon_{\text{DI}}| \leq 1.9 \cdot 10^{-16+\alpha}$. This relation shows that the CP asymmetry could escape the DI bound without causing the contradiction with the neutrino oscillation data if $|\lambda_5|$ and M_1 take suitable values. In order to fix the values of neutrino Yukawa couplings, we impose the neutrino oscillation data in the same way as in the previous examples with $q_1 = 0.85$, $q_2 = -0.27$, and $q_3 = 2.4$. For such neutrino Yukawa couplings, we obtain $\sin^2 2\theta_{13} = 0.085$ independently on the value of $|\lambda_5|$. The baryon number asymmetry Y_B obtained at $z = 20$ through the analysis of the Boltzmann equations is plotted for some typical values of $|\lambda_5|$ and M_1 in the left panel of Fig. 5. Since this z is much smaller than $z_{\text{EW}} = \frac{M_1}{T_{\text{EW}}}$, $Y_B(\infty)$ could be much smaller than the plotted value if the washout effects do not decouple. However, we can confirm that the plotted Y_B is recognized as $Y_B(\infty)$, at least for $|\lambda_5| > |\lambda_5^{\text{max}}|$, where $|\lambda_5^{\text{max}}|$ gives the maximum value of Y_B . In the region of $|\lambda_5| < |\lambda_5^{\text{max}}|$, the neutrino Yukawa couplings become large enough to continue reducing the generated lepton number asymmetry through the lepton number-violating scatterings which do not decouple at $z = 20$ completely. Since $|h_{2,3}|$ is required to be larger for the smaller values of $|\lambda_5|$ from the neutrino oscillation data, the large part of the generated lepton number asymmetry is considered to be washed out effectively although a larger $|\varepsilon|$ value is expected. The figure shows that the required value of Y_B is generated for $M_1 > 10^8 \text{ GeV}$, which is somewhat smaller than the one required in the ordinary seesaw case.¹¹

¹¹The required baryon number asymmetry could be generated even in the case with $M_1 = O(10^8) \text{ GeV}$ if special texture for the neutrino mass matrix is assumed even in the ordinary seesaw case [26].

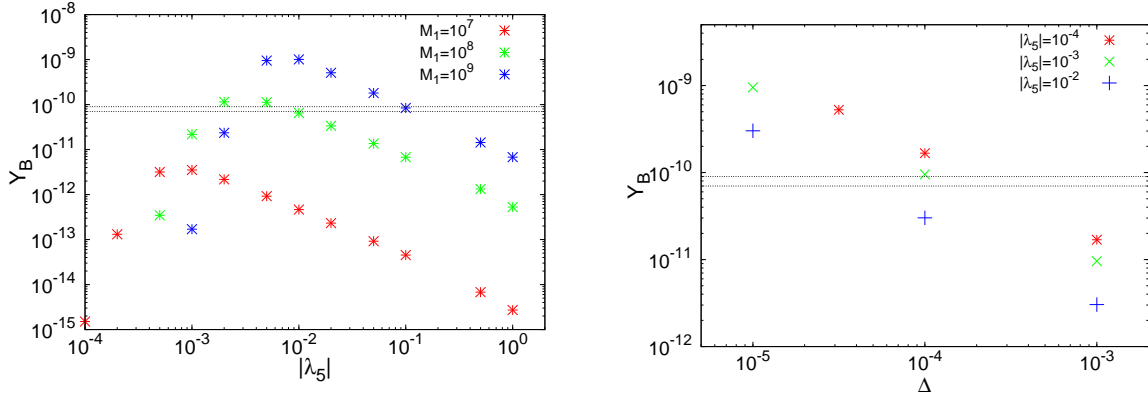


Fig. 5 The baryon number asymmetry Y_B in cases of the heavy right-handed neutrinos (the left panel) and the degenerate right-handed neutrinos (the right panel). In the left panel, a GeV unit is used for the mass scale. In the right panel, $M_1 = 2$ TeV is assumed.

3.2 Improvement by suppressing the washout

In the previous part we found that it is difficult to generate the sufficient baryon number asymmetry in consistent with all the neutrino oscillation data and the DM direct search as long as the mass of the lightest right-handed neutrino is assumed in a TeV range. This result is considered to be brought about by the large washout effect of the generated lepton number asymmetry. Here, we consider a possible improvement of this situation by making the neutrino Yukawa couplings small enough to suppress the washout. In this improvement, the CP asymmetry $|\varepsilon|$ should be kept to a suitable value such as $O(10^{-7})$ or more, simultaneously. Resonant leptogenesis can realize it.

As such an example, we suppose that the right-handed neutrino masses M_1 and M_2 are nearly degenerate in case (ia). M_1 is fixed to 2 TeV and M_2 is replaced with $M_2 = (1 + \Delta)M_1$. In this case, we can make the neutrino Yukawa couplings much smaller than the ones in case (ia) by assuming a larger value for $|\lambda_5|$. For instance, if we put $|\lambda_5| = 10^{-3}$, all the neutrino oscillation data can be satisfied for $|h_2| = 3.1 \cdot 10^{-4}$ and $|h_3| = 1.5 \cdot 10^{-4}$. Although the smaller neutrino Yukawa couplings tend to make the CP asymmetry $|\varepsilon|$ smaller, we can enhance $|\varepsilon|$ by supposing the degenerate right-handed neutrino masses. On the other hand, in that case the washout effect could be suppressed sufficiently. In the usual resonant leptogenesis with the right-handed neutrino masses at TeV regions [22, 27, 28], the generation of the sufficient lepton number asymmetry requires rather strict mass degeneracy. We examine whether this situation can be changed in this

neutrino mass generation scenario.

In the nearly degenerate right-handed neutrino case, the dominant contribution to the CP asymmetry in the decay of N_1 comes from the interference between the tree and the self-energy diagrams.¹² In the present case, the CP asymmetry $|\varepsilon|$ can be expressed as [22, 27, 28]

$$\begin{aligned} \varepsilon &= \sum_{i=2,3} \frac{\text{Im}(h^\dagger h)_{1i}^2}{(h^\dagger h)_{11}(h^\dagger h)_{ii}} \frac{(M_1^2 - M_i^2)M_1\Gamma_i}{(M_1^2 - M_i^2)^2 + M_1^2\Gamma_i^2} \\ &\simeq \frac{(M_1^2 - M_2^2)M_1\Gamma_2}{(M_1^2 - M_2^2)^2 + M_1^2\Gamma_2^2} \sin 2(\varphi_1 - \varphi_2) \simeq -\frac{2\Delta\tilde{\Gamma}_2}{4\Delta^2 + \tilde{\Gamma}_2^2} \sin 2(\varphi_1 - \varphi_2), \end{aligned} \quad (32)$$

where $\tilde{\Gamma}_2 = \frac{|h_2|^2}{4\pi}(1 + q_1^2) \left(1 - \frac{M_2^2}{M_1^2}\right)^2$. For case (ia) with $\sin 2(\varphi_1 - \varphi_2) = O(1)$, $|\varepsilon|$ can have a value of $O(1)$ for $\Delta \sim 5 \cdot 10^{-7}$. Thus, we can expect that the mass degeneracy required to bring about the sufficient baryon number asymmetry could be much milder than the usually assumed value $\Delta \lesssim 10^{-8}$ in the TeV-scale resonant leptogenesis [28].

We use the formula for ε given above and estimate Y_B by solving the Boltzmann equations in eq. (29) for some typical values of Δ by varying the value of $|\lambda_5|$. In the right panel of Fig. 5, we plot the numerical results of the obtained baryon number asymmetry. The required baryon number asymmetry is found to be generated for the right-handed neutrinos with the mass degeneracy $\Delta = O(10^{-4})$ for each value of $|\lambda_5|$. This degeneracy is much milder in comparison with the ordinary resonant leptogenesis at TeV scales. The result is caused by the nature of the model such that the neutrino Yukawa couplings can take sufficiently small values to suppress the washout effect keeping the neutrino masses in the appropriate range for the explanation of the neutrino oscillation data. The freedom of λ_5 makes it possible. The present neutrino mass generation scheme can give the consistent explanation for the three phenomenological problems in the SM if only the rather mild mass degeneracy between two light right-handed neutrinos is assumed without large extension of the model.

¹²Since the Yukawa couplings of $N_{2,3}$ are required to be much larger than $|h_1| = 3 \cdot 10^{-8}$ for N_1 , $N_{2,3}$ are considered to be in the thermal equilibrium. Thus, we can not expect a substantial contribution to the lepton number asymmetry from the decays of $N_{2,3}$.

4 Summary

The inert doublet model extended with the right-handed neutrinos is a simple and interesting framework for both neutrino masses and dark matter. In this scenario, the lightest right-handed neutrino or the lightest neutral component of the inert doublet can be a dark matter candidate. Since the neutrino Yukawa couplings should be $O(1)$ to reduce the relic abundance of dark matter in the former case, the thermal leptogenesis is difficult due to the strong washout effect. On the other hand, the neutrino Yukawa couplings can be irrelevant to the dark matter abundance in the latter case. Thus, the latter scenario has been considered to give the consistent explanation for the origin of the small neutrino masses, the existence of dark matter and the baryon number asymmetry in the Universe.

In this paper, we reexamined the possibility for the simultaneous explanation of these three problems in the latter case. We took account of the quantitative explanation for all the neutrino oscillation data including the recent results for $\sin^2 2\theta_{13}$ in the analysis. The results of our study suggest that the sufficient amount of baryon number asymmetry seems not to be generated in a consistent way with the full neutrino oscillation data. The neutrino Yukawa couplings could be large enough to enhance the CP asymmetry even for the $O(1)$ TeV right-handed neutrinos in the consistent way with the neutrino oscillation data by using the freedom of λ_5 . However, the same Yukawa couplings induce the lepton number-violating scattering processes to wash out the generated lepton number asymmetry. We checked this point through the numerical study. Although we do not study the whole parameter space, this feature seems to be rather general and then it seems not so easy to find the parameters to escape this situation without any modification.

We also examined the same problem in the modified situation such as the case with the heavy right-handed neutrinos like the ordinary type I seesaw and also the case with the degenerate light right-handed neutrinos. In the former case, we found that the right-handed neutrino could be somewhat lighter than the ordinary seesaw one but needs to be heavy enough to the similar level to it. In the latter case, even if the right-handed neutrino masses are in a TeV range, the resonant effect can enhance the CP asymmetry to generate the sufficient amount of baryon number asymmetry even for the small neutrino Yukawa couplings which can suppress the washout sufficiently. An interesting point is that the required mass degeneracy in this case is much milder than the one in the ordinary seesaw case. This possibility is brought about by the characteristic feature in this inert doublet

model with the radiative neutrino mass generation. More complete study of the parameter regions which are not searched in this paper will be presented in future publication.

Acknowledgement

This work is partially supported by Grant-in-Aid for Scientific Research (C) from Japan Society for Promotion of Science (No. 21540262 and No. 24540263), and also a Grant-in-Aid for Scientific Research on Priority Areas from The Ministry of Education, Culture, Sports, Science and Technology (No. 22011003).

Appendix

In this Appendix, we give the formulas of the reaction density contributing to the Boltzmann equations for the number density of N_1 and the lepton number asymmetry. For the processes relevant to their evolution, we could refer to the reaction density given in [24]. In the present model, however, interaction terms of η and N_1 are restricted by the Z_2 symmetry and also the masses of η and N_i take the similar order values, which cause large difference from the ordinary seesaw leptogenesis. Thus, we need to modify these formulas by taking account of the features of the present model.¹³

In order to give the expression for the reaction density of the relevant processes, we introduce dimensionless variables

$$x = \frac{s}{M_1^2}, \quad a_j = \frac{M_j^2}{M_1^2}, \quad a_\eta = \frac{M_\eta^2}{M_1^2}, \quad (33)$$

where s is the squared center of mass energy. The reaction density for the decay of N_1 can be expressed as

$$\gamma_D^{N_1} = \frac{(1 + q_1^2)|h_1|^2}{4\pi^3} M_1^4 (1 - a_\eta)^2 \frac{K_1(z)}{z}, \quad (34)$$

where $K_1(z)$ is the modified Bessel function of the first kind.

The reaction density for the scattering processes is expressed as

$$\gamma(ab \rightarrow ij) = \frac{T}{64\pi^4} \int_{s_{\min}}^{\infty} ds \hat{\sigma}(s) \sqrt{s} K_1\left(\frac{\sqrt{s}}{T}\right), \quad (35)$$

where $s_{\min} = \max[(m_a + m_b)^2, (m_i + m_j)^2]$ and $\hat{\sigma}(s)$ is the reduced cross section. In order to give the expression for the reaction density of the processes relevant to eq. (29), we define the following quantities for convenience:

$$\begin{aligned} \frac{1}{D_i(x)} &= \frac{x - a_i}{(x - a_i)^2 + a_i^2 c_i}, & c_i &= \frac{1}{16\pi^2} \left(\sum_{k=e,\mu,\tau} |h_{ki}|^2 \right)^2 \left(1 - \frac{a_\eta}{a_i} \right)^4, \\ \lambda_{ij} &= [x - (\sqrt{a_i} + \sqrt{a_j})^2] [x - (\sqrt{a_i} - \sqrt{a_j})^2], \\ L_{ij} &= \ln \left[\frac{x - a_i - a_j + 2a_\eta + \sqrt{\lambda_{ij}}}{x - a_i - a_j + 2a_\eta - \sqrt{\lambda_{ij}}} \right], \\ L'_{ij} &= \ln \left[\frac{\sqrt{x}(x - a_i - a_j - 2a_\eta) + \sqrt{\lambda_{ij}}(x - 4a_\eta)}{\sqrt{x}(x - a_i - a_j - 2a_\eta) - \sqrt{\lambda_{ij}}(x - 4a_\eta)} \right]. \end{aligned} \quad (36)$$

¹³Although the modified ones are given in Appendix of [12], the mass spectrum assumed there is different from the present one. The following formulas are arranged to applicable to the scenario in this paper.

As the lepton number violating scattering processes induced through the N_i exchange, we have

$$\begin{aligned}
\hat{\sigma}_N^{(2)}(x) &= \frac{1}{2\pi} \frac{(x - a_\eta)^2}{x^2} \left[\sum_{i=1}^3 (hh^\dagger)_{ii}^2 \frac{a_i}{x} \left\{ \frac{x^2}{xa_i - a_\eta^2} + \frac{2x}{D_i(x)} + \frac{(x - a_\eta)^2}{2D_i(x)^2} \right. \right. \\
&- \left. \frac{x^2}{(x - a_\eta)^2} \left(1 + \frac{2(x + a_i) - 4a_\eta}{D_i(x)} \right) \ln \left(\frac{x(x + a_i - 2a_\eta)}{xa_i - a_\eta^2} \right) \right\} \\
&+ \sum_{i>j} \text{Re}[(hh^\dagger)_{ij}^2] \frac{\sqrt{a_i a_j}}{x} \left\{ \frac{x}{x - a_i} + \frac{x}{x - a_j} + \frac{(x - a_\eta)^2}{(x - a_i)(x - a_j)} \right. \\
&+ \frac{x^2}{(x - a_\eta)^2} \left(\frac{2(x + a_i - 2a_\eta)}{a_j - a_i} - \frac{x + a_i - 2a_\eta}{x - a_j} \right) \ln \frac{x(x + a_i - 2a_\eta)}{xa_i - a_\eta^2} \\
&\left. \left. + \frac{x^2}{(x - a_\eta)^2} \left(\frac{2(x + a_j - 2a_\eta)}{a_i - a_j} - \frac{x + a_j - 2a_\eta}{x - a_i} \right) \ln \frac{x(x + a_j - 2a_\eta)}{xa_j - a_\eta^2} \right\} \right] \quad (37)
\end{aligned}$$

for $\ell_\alpha \eta^\dagger \rightarrow \bar{\ell}_\beta \eta$ and also

$$\begin{aligned}
\hat{\sigma}_N^{(13)}(x) &= \frac{1}{2\pi} \left[\sum_{i=1}^3 (hh^\dagger)_{ii}^2 \left\{ \frac{a_2(x^2 - 4xa_\eta)^{1/2}}{a_i x + (a_i - a_\eta)^2} \right. \right. \\
&+ \left. \frac{a_i}{x + 2a_i - 2a_\eta} \ln \left(\frac{x + (x^2 - 4xa_\eta)^{1/2} + 2a_i - 2a_\eta}{x - (x^2 - 4xa_\eta)^{1/2} + 2a_i - 2a_\eta} \right) \right\} \\
&\left. + \sum_{i>j} \frac{\text{Re}[(hh^\dagger)_{ij}^2] \sqrt{a_i a_j}}{x + a_i + a_j - 2a_\eta} \ln \left(\frac{x + (x^2 - 4xa_\eta)^{1/2} + a_i + a_j - 2a_\eta}{x - (x^2 - 4xa_\eta)^{1/2} + a_i + a_j - 2a_\eta} \right) \right] \quad (38)
\end{aligned}$$

for $\ell_\alpha \ell_\beta \rightarrow \eta\eta$. Here we note that cross terms has no contribution if the maximum CP phases are assumed in the way as $\sin 2(\varphi_{2,3} - \varphi_1) = 1$ with $\varphi_1 = 0$. We adopt this possibility in the numerical analysis, for simplicity. Since another type of lepton number violating processes $N_i N_j \rightarrow \ell_\alpha \ell_\beta$ induced by the η exchange have additional suppression due to a small $|\lambda_5|$, we can neglect them safely.¹⁴

As the lepton number conserving scattering processes which contribute to determine the number density of N_1 , we have

$$\begin{aligned}
\hat{\sigma}_{N_i N_j}^{(2)}(x) &= \frac{1}{4\pi} \left[\sum_{i,j=1}^3 |(hh^\dagger)_{ii} (hh^\dagger)_{jj}| \frac{\sqrt{\lambda_{ij}}}{x} \left(1 + \frac{(a_i - a_\eta)(a_j - a_\eta)}{(a_i - a_\eta)(a_j - a_\eta) + xa_\eta} \right. \right. \\
&\left. \left. + \frac{a_i + a_j - 2a_\eta}{x} L_{ij} \right) - \text{Re}[(hh^\dagger)_{ij}^2] \frac{2\sqrt{a_i a_j} L_{ij}}{x - a_i - a_j + 2a_\eta} \right] \quad (39)
\end{aligned}$$

¹⁴We should note that $|\lambda_5|$ might not have a small value in the case with heavy right-handed neutrinos, which is discussed in section 3. In this case, these processes could give large contribution to the washout of the generated lepton number asymmetry.

for $N_i N_j \rightarrow \ell_\alpha \bar{\ell}_\beta$ which are induced through the η exchange and also

$$\begin{aligned} \hat{\sigma}_{N_i N_j}^{(3)}(x) &= \frac{1}{4\pi} \frac{(x - 4a_\eta)^{1/2}}{x^{1/2}} \left[|(hh^\dagger)_{ij}|^2 \left\{ \frac{\sqrt{\lambda_{ij}}}{x} \left(-2 \right. \right. \right. \\ &+ \left. \left. \frac{4a_\eta(a_i - a_j)^2}{(a_\eta - a_i)(a_\eta - a_j)x + (a_i - a_j)^2 a_\eta} \right) + \left(1 - 2\frac{a_\eta}{x} \right) L'_{ij} \right\} \\ &- \left. \left. \text{Re}[(hh^\dagger)_{ij}^2] \left(\frac{\sqrt{\lambda_{ij}}}{x} + \frac{2(a_\eta^2 - a_i a_j) L'_{ij}}{(x^2 - 4xa_\eta)^{1/2}(x - a_i - a_j - 2a_\eta)} \right) \right] \right] \quad (40) \end{aligned}$$

for $N_i N_j \rightarrow \eta\eta^\dagger$ which are induced through the ℓ_α exchange. The cross terms in these reduced cross sections are neglected because of the same reasoning as eqs (37) and (38).

In order to see the behavior of these relevant processes such as the decoupling time, we may estimate the ratio of the reaction rate to the Hubble rate $\frac{\Gamma}{H}$ as a function of z (see Fig. 3). The thermally averaged reaction rate Γ is related to the above discussed reaction densities through

$$\Gamma_D^{N_1} = \frac{\gamma_D^{N_1}}{n_{N_1}^{\text{eq}}} \quad (41)$$

for the decay of N_1 and also

$$\Gamma_N^{(2,13)} = \frac{\gamma_N^{(2,13)}}{n_\ell^{\text{eq}}}, \quad \Gamma_{N_i N_1}^{(2,3)} = \frac{\gamma_{N_i N_1}^{(2,3)}}{n_{N_{R_1}}^{\text{eq}}} \quad (42)$$

for the 2-2 scattering processes given in eqs. (37), (38) and eqs. (39), (40), respectively.

References

- [1] Super-Kamiokande Collaboration, Y. Fukuda, *et al.*, Phys. Rev. Lett. **81** (1998) 1562; SNO Collaboration, Q. R. Ahmad, *et al.*, Phys. Rev. Lett. **89** (2002) 011301; KamLAND Collaboration, K. Eguchi, *et al.*, Phys. Rev. Lett. **90** (2003) 021802; K2K Collaboration, M. H. Ahn, *et al.*, Phys. Rev. Lett. **90** (2003) 041801.
- [2] WMAP Collaboration, D. N. Spergel, *et al.*, Astrophys. J. **148** (2003) 175; SDSS Collaboration, M. Tegmark, *et al.*, Phys. Rev. **D69** (2004) 103501.
- [3] A. Riotto and M. Trodden, Ann. Rev. Nucl. Part. Sci. **49** (1999) 35; W. Bernreuther, Lect. Notes Phys. **591** (2002) 237; M. Dine and A. Kusenko, Rev. Mod. Phys. **76** (2003) 1.
- [4] E. Ma, Phys. Lett. **B625** (2005) 76.
- [5] R. Barbieri, L. J. Hall and V. S. Rychkov, Phys. Rev. **D74** (2006) 015007; M. Cirelli, N. Fornengo and A. Strumia, Nucl. Phys. **B753** (2006) 178; L. L. Honorez, E. Nezri, J. F. Oliver and M. H. G. Tytgat, JCAP **0702** (2007) 028; Q.-H. Cao and E. Ma, Phys. Rev. **D76** (2007) 095011; S. Andreas, M. H. G. Tytgat and Q. Swillens, JCAP **0904** (2009) 004; E. Nezri, M. H. G. Tytgat and G. Vertongen, JCAP **0904** (2009) 014; L. L. Honorez, JCAP **1101** (2011) 002; M. Gustafsson, S. Rydbeck, L. L. Honorez, and E. Lundström, arXiv:1206.6316 [hep-ph].
- [6] T. Hambye, F.-S. Ling, L. L. Honorez and J. Roche, JHEP **0907** (2009) 090.
- [7] E. Ma, Mod. Phys. Lett. **A21** (2006) 1777.
- [8] D. T.-Smith and N. Weiner, Phys. Rev. **D72** (2005) 063509; S. Chang, G. D. Kribs, D. T.-Smith and N. Weiner, Phys. Rev. **D79** (2009) 043513
- [9] Y. Cui, D. E. Marrissey, D. Poland and L. Randall, JHEP **0905** (2009) 076; C. Arina, F.-S. Ling and M. H. G. Tytgat, JCAP **0910** (2009) 018.
- [10] E. Ma, Phys. Rev. **D73** (2006) 077301; J. Kubo, E. Ma and D. Suematsu, Phys. Lett. **B642** (2006) 18; J. Kubo and D. Suematsu, Phys. Lett. **B643** (2006) 336; D. Aristizabal Sierra, J. Kubo, D. Restrepo, D. Suematsu and O. Zapata, Phys. Rev.

- D79** (2009) 013011; D. Suematsu, T. Toma and T. Yoshida, Phys. Rev. **D79** (2009) 093004; D. Suematsu, T. Toma and T. Yoshida, Phys. Rev. **D82** (2010) 013012.
- [11] H. Fukuoka, J. Kubo and D. Suematsu, Phys. Lett. **B678** (2009) 401; D. Suematsu and T. Toma, Nucl. Phys. **B847** (2011) 567; H. Fukuoka, D. Suematsu and T. Toma, JCAP **07** (2011) 001.
- [12] D. Suematsu, Eur. Phys. J **C72** (2012) 72.
- [13] D. Suematsu, Eur. Phys. J. **C56** (2008) 379; H. Higashi, T. Ishima and D. Suematsu, Int. J. Mod. Phys. **A26** (2011) 995; D. Suematsu, Phys. Rev. **D85** (2012) 073008.
- [14] T2K Collaboration, K. Abe, *et al.*, Phys. Rev. Lett. **107** (2011) 041801; Double Chooz Collaboration, Y. Abe, *et al.*, Phys. Rev. Lett. **108** (2012) 131801; RENO Collaboration, J. K. Ahn, *et al.*, Phys. Rev. Lett. **108** (2012) 191802; The Daya Bay Collaboration, F. E. An, *et al.*, Phys. Rev. Lett. **108** (2012) 171803.
- [15] K. Griest and D. Seckel, Phys. Rev. **D43** (1991) 3191; P. Gondolo and G. Gelmini, Nucl. Phys. **B360** (1991) 145.
- [16] D. Tucker-Smith and N. Weiner, Phys. Rev. **D64** (2001) 043502.
- [17] CDMS Collaboration, Z. Ahmed, *et al.*, Phys. Rev. Lett. **102** (2009) 011301; XENON100 Collaboration, E. Aprile, *et al.*, Phys. Rev. Lett. **105** (2010) 131302.
- [18] G. Angloher *et al.*, Astropart. Phys. **31** (2009) 270; V. N. Lebedenko *et al.*, Phys. Rev. **D80** (2009) 052010.
- [19] K. Nakamura *et al.* (Particle Data Group), J. Phys. G **37** (2010) 075021.
- [20] T. Schwetz, M. Tórtola and J. Valle, New. J. Phys. **10** (2008) 113011; arXiv:1103.0734.
- [21] M. Fukugita and T. Yanagida, Phys. Lett. **B174** (1986) 45.
- [22] A. Pilaftsis, Phys. ReV. **D56** (1997) 5431.
- [23] E. W. Kolb and S. Wolfram, Nucl. Phys. **B172** (1980) 224; E. W. Kolb and M. S. Turner, *The Early Universe* (Addison-Wesley, Redwood City, CA, 1990).

- [24] M. Luty, Phys. Rev. **D45** (1992) 455; M. Plumacher, Nucl. Phys. **B530** (1998) 207.
- [25] S. Davidson and A. Ibarra, Phys. Lett. **B535** (2002) 25.
- [26] T. Baba and D. Suematsu, Phys. Rev. **D71** (2005) 073005.
- [27] M. Flanz, E. A. Pascos and U. Sarkar, Phys. Lett. **B345** (1995) 248; L. Covi, E. Roulet and F. Vissani, Phys. Lett. **B384** (1996) 169; E. Akhmedov, M. Frigerio and A. Yu Smirnov, JHEP **0309** (2003) 021; C. H. Albright and S. M. Barr, Phys. Rev. **D69** (2004) 073010; T. Hambye, J. March-Russell and S. W. West, JHEP **0407** (2004) 070.
- [28] A. Pilaftsis and E. J. Underwood, Nucl. Phys. **B692** (2004) 303; A. Pilaftsis and E. J. Underwood, Phys. Rev. **D72** (2005) 113001.